Seismic retrofit of square RC columns with polyethylene terephthalate (PET) fibre reinforced polymer composites

Jian-Guo Dai [a,*], Lik Lam [b], Tamon Ueda [c]

[a] *Department of Civil and Structural Engineering, The Hong Kong Polytechnic University, Hung Hom, Kowloon, Hong Kong, China*
[b] *Faculty of Construction and Land Use, The Hong Kong Polytechnic University, Hung Hom, Kowloon, Hong Kong, China*
[c] *Division of Built Environment, Faculty of Engineering, Hokkaido University, Kita-ku, Sapporo 060-8628, Japan*

ABSTRACT

This paper presents an experimental study on the seismic retrofit of reinforced concrete (RC) square columns with polyethylene terephthalate (PET) fibre reinforced polymer (FRP) composites, which is a new type of FRP with a larger tensile capacity compared to conventional FRPs. Test results of six PET FRP jacketed specimens are presented and compared with those of a specimen with high strength aramid FRP (HS AFRP) and two reference specimens. Hysteretic responses and failure modes of the specimens under a constant axial load and cyclic lateral loads, as well as the responses of the internal steel reinforcement and the FRP jackets are discussed in detail. The contributions of shear deformation and fixed end rotation due to the slip of longitudinal steel bars to the lateral displacement of columns are also investigated. The results show that PET FRP is a promising alternative to conventional FRPs for the seismic retrofit of RC columns. It improves the displacement ductility of RC columns significantly and does not rupture at the ultimate limit state. Future studies should examine a wider range of geometry and material properties and they should also be concerned with a systematic and direct comparison between specimens jacketed with PET FRP and conventional FRP with equivalent jacket stiffness.

© 2011 Elsevier Ltd. All rights reserved.

1. Introduction

The use of fibre reinforced polymer (FRP) composites as an external reinforcement has been a very effective means for the strengthening and seismic retrofit of reinforced concrete (RC) structures in the recent two decades. For the seismic retrofit of RC columns, FRP composites are used as external jackets with the main fibres running in the hoop direction. The seismic resistance of an RC column is significantly improved with FRP jacketing, because of the additional shear capacity and the lateral confinement to concrete [1–11].

Carbon FRP (CFRP) and glass FRP (GFRP) are among the most commonly used FRPs in strengthening and seismic retrofit applications, although aramid FRP (AFRP) has also been used. These three types of FRP composites are referred to as conventional FRPs in this paper. The stress–strain behaviour of conventional FRPs is linear elastic, with an ultimate tensile rupture strain around 1.5% for carbon FRP (CFRP), 2% for glass FRP (GFRP) and 3% for aramid FRP (AFRP). The ultimate limit state of conventional FRP-jacketed RC columns is often governed by FRP rupture [12,13], because of the small strain capacity and linear elastic nature of conventional FRPs. The mode of column failure by FRP rupture is brittle, which may be

accompanied with explosive failure of concrete [14–16] and rapid buckling of longitudinal steel reinforcement [4].

New types of FRP composites have recently appeared due to the availability of polyacetal fibres [16,17], polyethylene naphthalate (PEN) fibres and polyethylene terephthalate (PET) fibres [18], which are recycled materials from scrap polymer products. These new typical FRPs feature with much lower tensile stiffness but much larger strain capacities compared to conventional FRP composites, which will be referred to as large rupture strain FRPs in this paper. A comparison between conventional FRPs and the new types of FRPs, is given in Fig. 1.

An experimental investigation on the use of such large strain FRPs in the seismic retrofit of RC columns was conducted at Hokkaido University and Mitsui Sumitomo Research Centre, Japan [19]. The experimental program covered 15 RC columns with a square section of 400×400 mm or 600×600 mm. Thirteen of the columns were jacketed respectively with either PET FRP, PEN FRP or high strength (HS) AFRP in the plastic hinge zones, and high modulus (HM) AFRP outside the plastic hinge zones. The remaining two columns were tested as the reference specimens without any FRP. The specimens were designed in the context of seismic retrofit of RC bridge piers and were tested under a constant axial load and cyclic lateral load.

While a general description of the test results was provided in Anggawidjaja et al. [19], a detailed discussion on the strain and
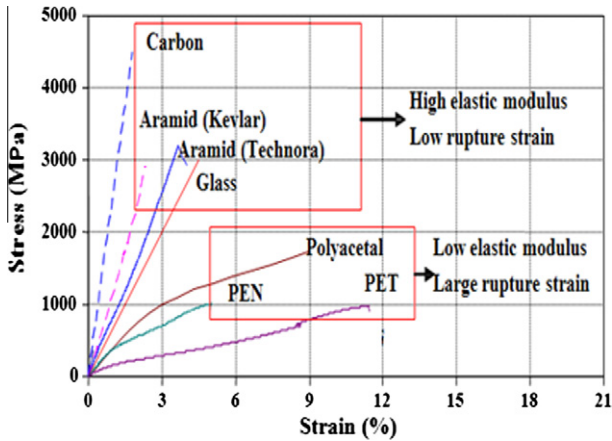
Fig. 1. Tensile stress–strain curves of various FRP materials.

displacement measurements was not. As a result, the unique properties of large rupture strain FRPs as compared with conventional FRPs have not been thoroughly explored. This paper is therefore focused on PET FRP-jacketed specimens of the above-mentioned tests, and only the specimens with a column section of 400×400 mm will be discussed. Detailed information with be provided on the hysteretic responses and failure modes of six PET FRP-jacketed specimens, one HS AFRP-jacketed specimen, and two reference specimens without any FRP. A comprehensive set of data on the strain responses in internal steel reinforcements and FRP jackets, which have not been provided in Anggawidjaja et al. [19], will also be presented. As a result, the development of strains in PET FRP jackets at different loading stages will be discussed. In addition, the effects of shear deformation and fixed end rotation due to the slip of longitudinal steel bars to the lateral displacement of columns will also be explored, based on more stringent assumptions and the availability of extensive data from strain and displacement measurements.

2. Experimental details

The specimens to be discussed in this paper include seven retrofitted specimens and two reference specimens without use of any FRP. The retrofitted specimens were jacketed with HM AFRP outside the plastic hinge zone, with either PET FRP

(six specimens) or HS AFRP (one specimen) in the plastic hinge zone. These specimens were tested in two batches which were differentiated by differing shear spans of 1150 mm and 1500 mm (see Table 1). Each specimen consisted of a square column whose corners were chamfered with a width of 25 mm, and an RC column of 600-mm thick (the footing) which was cast monolithically, as shown in Fig. 2. The columns were reinforced longitudinally with steel bars of 16 mm in diameter and transversely with steel bars of 6 mm in diameter. The longitudinal steel bars were anchored into the footing with a sufficient anchorage length. The yield strength of the longitudinal steel bars was 394 MPa and that of the transverse steel bars was 383 MPa. The concrete had the cylinder compressive strengths of 29.4 MPa for specimens SP-1 to SP-4, and 31.7 MPa for other specimens, at the age of 28 days. The material properties of HS AFRP, PET FRP, and HM AFRP, as provided by material suppliers, are given in Table 2.

All the specimens were tested under a constant axial compression load of 160 kN and reversed cyclic lateral loads at increasing target displacement levels. The constant axial load was applied using a vertically aligned hydraulic jack, which represented the dead loads of the super structures on a bridge. The lateral load was applied using a horizontally aligned hydraulic actuator which was operated manually in a displacement control mode. The first load cycle was targeted at the first yield of the longitudinal reinforcement, which was identified by monitoring the strains in the reinforcement. The target displacement was increased by a displacement value equaling to the yield displacement δ_y for each subsequent cycle. The history of lateral loading is shown in Fig. 3.

During the tests, the axial and lateral loads were monitored using load cells. The horizontal displacements were measured using linear variable differential transformers (LVDTs). For specimens SP-5 to SP-10, an additional set of five LVDTs were used to measure the shear deformation of the column within the plastic hinge region, as schematized in Fig. 4. A large number of strain gauges (with a gauge length of 5 mm) were installed in each specimen to measure the strains in the longitudinal and transverse steel bars, and in the FRP jackets. The distribution of strain gauges is shown in Fig. 2.

3. Hysteretic responses and failure modes

The key results of the tests, including the lateral load and displacement at the first yield (P_y and δ_y), the maximum load (P_{max}), flexural strength M_u and the displacement ductility factor μ_ε (i.e., ratio between the ultimate displacement δ_u and the first yield displacements δ_y), are given in Table 1. The ultimate displacement δ_u was defined as that at which a drop of the load from P_{max} to P_y was experienced. Theoretical values of M_u, μ_ε and shear strength V_u based on the JSCE provisions [20] are also provided for comparison. The hysteretic load–displacement responses of the specimens are shown in Figs. 5 and 6 for specimens with the shear spans of 1150 mm and 1500 mm, respectively. The yield of longitudinal reinforcement, the yield of transverse reinforcement, the buckling of longitudinal reinforcement and the rupture of FRP jacket, are marked as "1", "2", "3" and "4" on the figures, respectively. The

Table 1
Summary of test specimens.

Items		Specimen								
		SP-1	SP-2	SP-4	SP-5	SP-6	SP-7	SP-8	SP-9	SP-10
Shear span a (mm)				1150				1500		
Concrete strength f_c' (MPa)			29.4					31.7		
Longitudinal steel				5Φ19					6Φ19	4Φ19
Transverse steel					Φ6 at 100					
Type of fibre	Outside PHZ				HM-A				HM-A	
	Within PHZ		HS-A			PET			PET	
Thickness of FRP t_f (mm)	Outside PHZ	0	0.194	0.194	0.097	0.048	0.048	0	0.048	0.048
	Within PHZ	0	0.252	0.750	0.374	0.249	0.125	0	0.249	0.125
[*]Predicted M_u (kN m)		331	331	331	334	334	334	334	410	265
[*]Predicted V_u	Outside PHZ	230	461	461	364	301	301	234	315	297
	Within PHZ	230	443	443	324	294	264	234	308	260
[*]Predicted $\mu_\varepsilon = \delta_u/\delta_y$		4.3	5.79 [#](7.01)	9.96	N.A	7.62	6.35	4.39	6.97	7.48
Test results	δ_y (mm)	6.14	6.19	6.20	6.73	9.64	9.57	10.0	10.4	8.07
	P_y (kN)	214.9	220.9	223.0	199.3	146.6	157.4	152.0	182.6	115.2
	P_{max} (kN)	309.8	290.6	306.3	297.9	228.3	230.7	225.8	269.9	178.0
	M_u (kN m)	356.2	334.2	352.2	342.6	342.5	346.1	338.7	404.4	267.0
	$\mu_\varepsilon = \delta_u/\delta_y$	2.7	11.8	11.4	9.2	9.4	8.5	7.2	8.8	11.0

[*] Predicted based on the JSCE (2001) provisions.
[#] Predicted based on the material ultimate tensile strain of HS AFRP.